https://doi.org/10.5194/bg-2020-93
Preprint. Discussion started: 21 April 2020

Biogeosciences Discussions
Open Access
EGU

Uncertainties, sensitivities and robustness of simulated water erosion in an EPIC-based global-gridded crop model

Tony W. Carr[1,*], Juraj Balkovič[2,3], Paul E. Dodds[1], Christian Folberth[2], Emil Fulajtar[4], Rastislav Skalsky[2,5]

[1]University College London, Institute for Sustainable Resources, London, United Kingdom

[2] International Institute for Applied Systems Analysis, Ecosystem Services and Management Program, Laxenburg, Austria

[3] Department of Soil Science, Faculty of Natural Sciences, Comenius University in Bratislava, Bratislava, Slovak Republic

[4] International Atomic Energy Agency, Joint FAO/IAEA Division of Nuclear Techniques in Food and Agriculture, Vienna, Austria

[5] National Agricultural and Food Centre, Soil Science and Conservation Research Institute, Bratislava, Slovak Republic

* Correspondence to: Tony Carr (tony.carr.16@ucl.ac.uk)

Abstract. Water erosion in agricultural fields can reduce soil fertility and agricultural productivity. Despite the impact of water erosion on crops, it is typically neglected in global crop yield projections. Furthermore, previous efforts to quantify global water erosion have paid little attention to the effects of field management on the magnitude of water erosion. In this study, we analyse the robustness of simulated water erosion estimates in wheat and maize fields between the years 1980 to 2010 based on daily model outputs from a global gridded version of the Environmental Policy Integrated Climate (EPIC) crop model. Using the MUSS water erosion equation and country-specific and environmental indicators determining different intensities in tillage, residue handling and cover crops, we simulate global annual median and average water erosion rates of 6 t ha^{-1} and 19 t ha^{-1} and an annual soil removal of 7 Gt in global wheat and maize fields. A comparison of our simulation results with field data demonstrates an overlap of simulated and measured water erosion values for the majority of global cropland. Slope inclination and daily precipitation are key factors in determining the agreement between simulated and measured erosion values and are the most critical input parameters controlling all water erosion equations included in EPIC. The many differences between field management methods worldwide and the varying water erosion estimates from different equations add uncertainty to the simulation results. To reduce the uncertainties addressed here and to improve global water erosion estimates generally, more data on global field management and more field data from study sites representing the diversity of environmental conditions where crops are grown are necessary.

1 Introduction

Water erosion is widely recognized as a threat to global agriculture (den Biggelaar et al., 2004; Kaiser, 2004; Panagos et al., 2018; Pimentel, 2006). The removal of topsoil by surface runoff reduces soil fertility and crop

https://doi.org/10.5194/bg-2020-93
Preprint. Discussion started: 21 April 2020

yields due to loss of nutrients, degradation of the soil structure, and decreasing plant-available water capacity (Våje et al., 2005). Water erosion is a natural process, but the impact of agricultural field management on surface cover and roughness is decisive for the magnitude of water erosion. High energy precipitation, steep slopes and lack of vegetation cover intensify water erosion. The most vulnerable areas are mountainous regions, due to steep slopes, the tropics and subtropics, due to abundant high energy precipitation, and arid regions, where precipitation events are rare but often intense and the vegetation cover is sparse. Since agricultural cultivation of mountains and arid regions is limited, the most significant degradation of agricultural land by water erosion occurs in tropical areas. This global distribution of water erosion is indicated by suspended sediment in rivers (Walling and Webb, 1996). South America, Sub-Saharan Africa, South and East Asia have been identified as the most vulnerable regions to erosion on agricultural land by several prior studies (Borrelli et al., 2017; Pimentel et al., 1995).

Despite its importance for global agriculture, water erosion is usually not considered in global gridded crop model (GGCM) studies. Throughout the past decade, GGCMs - typically combinations of agronomic or ecosystems models and global gridded input data infrastructures - have become essential tools for climate change impact assessments, evaluations of agricultural externalities, and as input data providers for agro-economic models (Mueller et al., 2017). Few assessments have considered land degradation processes and found their inclusion and understanding crucial for evaluating climate change mitigation and adaptation strategies (Balkovič et al., 2018; Chappell et al., 2016). Beyond crop models, there is a need to improve the representation of agricultural management and soil-related processes in earth system models to better reflect carbon sinks and sources (Luo et al., 2016; McDermid et al., 2017; Pongratz et al., 2018). Yet, the necessary algorithms to simulate water erosion are often not incorporated in such models. Exceptions among field-scale crop models are the Environmental Policy Integrated Climate model (EPIC) and Agricultural Production Systems Simulator (APSIM), which are frequently used in GGCM ensemble studies. Compared to other commonly used crop models in GGCMs, EPIC stands out in its detailed representation of soil processes including water erosion and the impacts of tillage on soil properties (Folberth et al., 2019).

Recently, water erosion models such as the Universal Soil Loss Equation (USLE) and the Revised Universal Soil Loss Equation (RUSLE) have been used to estimate global water erosion. Annual global soil removal estimates and water erosion rates on cropland of recent studies range between 13 – 22 Gt and 11 - 13 t ha^{-1} (Borrelli et al., 2017; Doetterl et al., 2012; van Oost et al., 2007). USLE and its modifications were developed in the Midwestern United States and should ideally be evaluated against soil erosion measurements when used for other agro-environmental zones (Evans and Boardman, 2016). However, the uneven distribution and limited availability of field data around the world, the lack of long-term soil measurements and the great variability of the designs of erosion rate measurements hamper the evaluation of global soil loss estimates derived from models (Auerswald et al., 2004; Borrelli et al., 2017; García-Ruiz et al., 2015). In addition, model input data on topography, soil properties and land use are often aggregated over large areas and thus simulation results cannot be directly compared to single field measurements at specific locations.

Most global soil removal estimates using water erosion models are based on static observation approaches or on very coarse timescales that do not fall below annual time steps (Borrelli et al., 2017). Therefore, seasonal patterns of soil cover and precipitation intensities are neglected despite the fact that they are crucial factors for water erosion. The state of the soil and its cover is influenced by land management, such as the choice of crops, planting

https://doi.org/10.5194/bg-2020-93
Preprint. Discussion started: 21 April 2020

and harvest dates, tillage and plant residue management. Accordingly, neglecting the impact of seasonal changes in vegetation cover and field management practices constitutes large uncertainty in global water erosion estimates. Crop models usually simulate crop growth on a daily timescale, which allows attached water erosion models to account for daily changes in weather, soil properties and vegetation cover. However, uncertainty remains due to the increasing requirement of input data for daily simulations, which is especially challenging at a global scale.

In this study, we examine the uncertainties and sensitivities of water erosion estimates in an EPIC-based global-gridded crop model, and evaluate the robustness of large-scale simulation results against field-scale water erosion measurements aggregated from different world environments. We simulate global water erosion rates in wheat and maize fields using different empirical erosion equations in EPIC while accounting for the daily crop growth and development under different field management scenarios. Here, wheat and maize are used as representative crops of global agriculture, as they are grown under most environmental conditions and represent contrasting soil cover patterns. Our global simulations were carried out for a baseline crop management scenario based on a set of environmental and country-specific assumptions and indicators, which is a common practice in global gridded crop modelling. In addition to the baseline scenario we quantify the uncertainties of simulated water erosion values stemming from (i) uncertain field management inputs, and (ii) water erosion calculation methods. We also evaluate the model's sensitivity to all inputs involved in the water erosion calculation to interpret the variability and uncertainties of the simulation results, and to discuss the differences between water erosion equations. Finally, we use field measurements from various locations world-wide to evaluate the robustness of estimated water erosion rates under different environmental conditions.

2 Methods

The simplified framework in Figure 1 illustrates the particular stages of the methodological procedure applied by this study and their relationships to input data and model outputs. Both, input and output data are used twofold. We use input data i) to simulate daily wheat and maize growth and water erosion with EPIC, and ii) to analyse the sensitivity of relevant model parameters to simulate global water erosion with all equations in EPIC. We use model outputs i) to calculate a baseline global water erosion scenario, and ii) to address the uncertainty of simulation results. The final step of this study consists of the robustness check of the model outputs using field data. A detailed description of each element of this study is described in the following sections.

2.1 Modelling water erosion and crop growth with EPIC

2.1.1 Global gridded crop model and input data

We use a global gridded version of the Environmental Policy Integrated Climate (EPIC) crop model, EPIC-IIASA (Balkovič et al., 2014), to simulate soil sediment loss with runoff from 1980 to 2010 while accounting for the daily growth of maize and wheat under different field management scenarios. EPIC can simulate the growth of a wide range of crops and has a sophisticated representation of carbon, nutrient and water dynamics as well as a wide variety of possible field management options, including tillage operations and crop rotations (Izaurralde et al., 2006; Sharpley and Williams, 1990). Originally EPIC was named Erosion-Productivity Impact Calculator and was developed to determine the relationship between erosion and soil productivity. Due to its origin, EPIC has several options to calculate water erosion caused by precipitation, runoff and irrigation (Williams, 1990).

https://doi.org/10.5194/bg-2020-93
Preprint. Discussion started: 21 April 2020

EPIC-IIASA requires global soil and topography data and daily weather data. The basic spatial resolution of the model is 5' x 5' at which soil and topographic data are provided. These are aggregated to homogenous response units and further intersected with a 30' x 30' climate grid, the resolution at which global gridded climate data are available. This results in a total of 131,326 simulation units with a spatial resolution of 5' to 30' (about 9 km to 56 km near the equator). We run EPIC in each simulation unit upon a representative field with a defined slope length and field size based on a set of rules for different slope classes (Table S1). The slope class for each simulation unit is defined as the most common slope per simulation unit derived from a global terrain slope database (IIASA/FAO, 2012). We use global daily weather data from the AgMERRA dataset for the years 1980-2010 (Ruane et al., 2015), soil information from the Harmonized World Soil Database (FAO/IIASA/ISRIC/ISSCAS/JRC, 2009), and topography from USGS GTOPO30 (USGS, 1997). In each simulation unit, we consider reported growing seasons for maize and wheat (Sacks et al., 2010), and spatially explicit nitrogen and phosphorus fertilizer application rates (Mueller et al., 2012).

2.1.2 Water erosion equations

EPIC includes seven empirical equations to calculate water erosion (Wischmeier and Smith, 1978). The basic equation is:

$$Y = R * K * LS * C * P \quad (1)$$

where Y is soil erosion in Mg ha^{-1} (mass/area), R is the erosivity factor (erosivity unit/area), K is the soil erodibility factor in Mg MJ^{-1} (mass/erosivity unit), LS is the slope length and steepness factor (dimensionless), C is the soil cover and management factor (dimensionless) and P is the conservation practices factor (dimensionless).

The main difference between the water erosion equations available in EPIC is their energy components used to calculate the erosivity factor. The USLE, RUSLE and RUSLE2 equations use precipitation intensity as an erosive energy to calculate the detachment of soil particles. The Modified Universal Soil Loss Equation (MUSLE) equation and its variations MUST and MUSS use runoff variables to simulate water erosion and sediment yield. The Onstad-Foster equation (AOF) combines energy through rainfall and runoff (Table 1).

The erosion energy component is calculated as a function of either runoff volume Q (mm), peak runoff rate q_p (mm h^{-1}) and watershed area WSA (ha), or via the rainfall erosivity index EI (MJ ha^{-1}). The latter determines the detachment of soil particles through the energy of daily precipitation and a statistical estimate of the daily maximum intensity of precipitation falling within 30 minutes. RUSLE2 is the only equation calculating soil deposition. If the sediment load exceeds the transport capacity, determined by a function of flow rate and slope steepness, soil is deposited, which is calculated by a function of flow rate and particle size (USDA-ARC, 2013).

The soil cover and management factor is updated for every day where runoff occurs using a function of crop residues, biomass cover and surface roughness. The impact of soil erodibility on simulated water erosion is calculated for the top-soil layer at the start of each simulation year as a function of sand, silt, clay and organic carbon content. The topographic factor is calculated as a function of slope length and slope steepness. A detailed description of the cover and management, soil erodibility and topographic factor is provided in the supporting information (Text S1). The conservation practice factor is included in all equations as a static coefficient ranging between 0 and 1, where 0 represents conservation practices that prevent any erosion and 1 represents no

https://doi.org/10.5194/bg-2020-93
Preprint. Discussion started: 21 April 2020

conservation practices. Typical conservation practice factors can be derived from tables, which include values ranging from 0.01 to 0.35 for terracing strategies and from 0.25 to 0.9 for different contouring practices (Morgan, 2005; Wischmeier and Smith, 1978). Alternatively, values can be derived from local field studies and remote sensing (Karydas et al., 2009; Panagos et al., 2015), from equations using topographical data (Fu et al., 2005; Terranova et al., 2009), or from economic indicators (Scherer and Pfister, 2015).

2.1.3 Field management scenarios

Field management techniques influencing soil properties and soil cover have a significant impact on the amount of water erosion. However, these methods are very heterogenous around the world and data on different field management techniques are sparse. Therefore, three tillage management scenarios – conventional tillage, reduced tillage and no-tillage – were designed by altering parameters related to water erosion to analyse the impact of field management on simulated water erosion and to draw conclusions on its impact on the quality of simulation results.

In the reduced and no-tillage scenarios, we decrease soil disturbance by reducing cultivation operations, tillage depth and surface roughness, and we increase plant residues left in the field after harvest. In addition, we reduce the runoff curve numbers, which indicate the runoff potential of a hydrological soil group, land use and treatment class, with decreasing tillage intensification by using pre-defined values for the cover treatment classes presented in Table 2 (Sharpley and Williams, 1990). By lowering the runoff curve numbers, the impact of reduced tillage practices on the hydrologic balance can be taken into account (Chung et al., 1999). We simulate each tillage scenario with and without green fallow (grass) cover in between growing seasons, leading to a total of six field management scenarios.

2.2 Baseline scenario for estimating global water erosion in wheat and maize fields

We estimate the rate of water erosion globally by combining these six tillage and cover crop scenarios in different regions of the world, using climatic and country-specific assumptions and indicators (Table 3). We chose maize and wheat as two contrasting crop types for analysing water erosion in different cultivation systems. Maize is a row crop with relatively large areas of bare and unprotected soil between the crop rows. The plant density in wheat fields is much higher, which improves the protection of soils against water erosion.

We consider conventional and reduced tillage systems globally while considering no-tillage only for countries in which the share of conservation agriculture is at least 5 %. In tropical regions, we simulate water erosion with a grass cover in between maize and wheat seasons to account for soil cover from a year-round growing season. In temperate and snow regions, we simulate water erosion affected by both soil cover throughout the year and bare soil in winter seasons. In arid regions, we do not simulate grass cover in between growing seasons due to the limited water supply.

On slopes steeper than 5 %, we consider only rainfed agriculture, as hilly cropland is irrigated predominantly on terraces that prevent water runoff. To account for erosion control measures on steep slopes we use a conservation P-factor of 0.5 on slopes steeper than 16 % to simulate contouring, and P-factor of 0.15 on slopes steeper than 30 % to simulate terracing. The threshold for slopes that are cultivated with conservation practices is based on the slope classes used for the underlying structure of slope information of EPIC-IIASA, from which the three highest slope classes (16–30 %, 30–45 %, >45 %) mark slopes that are less likely to be cultivated without provisions to prevent erosion. We choose the MUSS equation for the baseline scenario as it generates the lowest deviation

https://doi.org/10.5194/bg-2020-93
Preprint. Discussion started: 21 April 2020

between simulated and measured water erosion as discussed below. Table 3 summarises the field management assumptions used in the baseline scenario.

2.3 Uncertainty analysis of field management scenarios and water erosion equations

Given the global scale of the analysis and the aggregated nature of available field management information, there is much uncertainty about crop management strategies, which introduces uncertainty in the water erosion estimates. In addition, each water erosion equation gives a different overall erosion estimate. To discuss the uncertainty of simulation results, we evaluate the variance in simulated water erosion rates at grid level due to: (i) different management assumptions, and (ii) the choice of water erosion equation. The variance of simulation outputs is defined as the range between minimum and maximum simulated water erosion rates with all combinations of tillage and cover crop scenarios and with each water erosion equation.

2.4 Sensitivity analysis of model parameters

We use a sensitivity analysis to identify the most essential input parameters to the factors in the seven water erosion equations. We use the Sobol method (Sobol, 1990), which is a variance-based sensitivity analysis that is popular in environmental modelling (Nossent et al., 2011). With this method, it is possible to quantify the amount of variance that each parameter contributes to the total variance of the model output. These amounts are expressed as sensitivity indices, which rank the importance of each input parameter for simulated water erosion. In addition, the sensitivity indices can be used to determine the impact of parameter interactions on the model output.

We test 30 parameters directly connected to the water erosion equations in EPIC. In total, we assign 126,976 random values to all input parameters along a pre-defined triangular distribution or a range of discrete values (Table S2). Water erosion is simulated with EPIC using the seven available equations for each random input combination at 40 locations where wheat and maize are cultivated. To represent a heterogenous distribution of global precipitation regimes, we use the natural break optimisation method to choose locations based on average annual precipitation amounts from 1980 to 2010 (Jenks, 1967). For each location and equation, the most sensitive parameters are ranked. To analyse the impact of precipitation regimes on the sensitivity of each parameter, we use Spearman coefficients (ρ) to determine if positive or negative relationships exist between each parameter's sensitivity and annual precipitation.

2.4 Evaluation of simulated erosion against reported field measurements

We compared our simulated water erosion rates with 473 soil erosion measurements from 39 countries; 314 records were derived by the ^{137}Cs method and 159 records from erosion plots. An overview of the field data is presented in Fig. S5-S8, and the full dataset is available in Table S5.

Guidance on the ^{137}Cs method is provided by Fulajtar et al. (2017); Mabit et al. (2014) and Zapata (2002). The ^{137}Cs radionuclide was released by nuclear weapon tests and from the accident of the Chernobyl Nuclear Power Plant to the atmosphere and subsequently deposited in the uppermost soil layer by atmospheric fallout. After its deposition it was bind to soil colloids and can be moved only together with soil particles by mechanical processes such as soil erosion. Its chemical mobility and uptake by plants is negligible (Mabit et al., 2014; Zapata, 2002). If part of the topsoil contaminated by ^{137}Cs is removed by erosion, the ^{137}Cs concentrations in soil profiles can be used to trace soil movements using mass balance equation (Walling et al., 2014). A major advantage of the ^{137}Cs method is that it provides long term mean erosion rates (representing the period since ^{137}Cs fallout in the 1960s

https://doi.org/10.5194/bg-2020-93
Preprint. Discussion started: 21 April 2020

until the time of sampling) and overcomes the problem of high temporal variability of erosion. Further advantages are that the obtained values are retrospective and that the erosion rates are determined for a grid of ^{137}Cs sampling points, which can provide valuable information on the spatial distribution of erosion.

To expand the field data records for evaluation, we use also erosion rate measurements from erosion plots collected by García-Ruiz et al. (2015). In contrast to the measurements using ^{137}Cs tracer, most plot measurements represent short-term erosion rates. Measurement periods span between 1 and 60 years with an average of 10 years.

The overwhelming effect of the experimental methodology on measured erosion rates in addition to the granular spatial resolution of our simulation setup hinders a direct comparison between simulated and observed water erosion rates. Instead we compare aggregated simulated and observed erosion values for different slope and precipitation classes to analyse the robustness of simulated water erosion rates under different environmental conditions. Therefore, only field measurements with recorded slope steepness and annual precipitation are used. Where annual precipitation amounts are not recorded, they are taken from the WorldClim2 dataset (Fick and Hijmans, 2017). Due to the non-normal distribution of the simulated and measured data, the median deviation (MD) is used as a measure to compare the agreement between simulated and measured water erosion values.

3 Results

We estimate global annual average and median water erosion rates in wheat and maize fields of 19 t ha^{-1} and 6 t ha^{-1} respectively (Fig. S3). The difference between these values indicates that the global average is influenced by extreme values. The total removal of soil in global wheat and maize fields is estimated to be 7 Gt a^{-1}. The map in Figure 2 illustrates the global distribution of simulated water erosion rates. Highest water erosion is simulated in mountainous regions and regions with strong precipitation, especially in tropical climate zones. In Asia, those regions are widespread in the east, south-east and the Himalaya region. In Africa, similar areas with high water erosion values are spread around the continent and are most common at the west coast and in East Africa including broad areas in Guinea, Sierra Leone, Liberia, Ethiopia and Madagascar. In South America, highest water erosion is simulated in the south of Brazil and regions around the Andes mountain range and the Amazon river basin. The highest water erosion values on the American continent were simulated in tropical Central America and the Caribbean. In North America, highest water erosion occurs along the west coast and in the east. Water erosion in Europe is highest in Mediterranean areas and around the Alps.

Median annual water erosion values for the five largest wheat and maize producing countries demonstrate the strong impact of climate and topography on simulated water erosion. In Brazil, China and India, where a large proportion of cropland is in tropical areas, water erosion is relatively high with annual median values of 10 t ha^{-1}, 6 t ha^{-1}, and 37 t ha^{-1}, respectively. In Russia and the United States annual median values are much lower with 1 t ha^{-1}, and 2 t ha^{-1}, respectively. Overall, Figure 2 illustrates the large variation in simulated water erosion between tropical climate regions and regions with a large proportion of flat and dry land.

3.1 Sources of model uncertainty related to management assumptions and method selection

The uncertainty of the simulation results due to management scenarios and the choice of water erosion equations is highest in regions most vulnerable to water erosion (Figure 3). The annual median uncertainty range at each

https://doi.org/10.5194/bg-2020-93
Preprint. Discussion started: 21 April 2020

grid due to management is 30 t ha^{-1}. For 97 % of grids, the lowest erosion rates are simulated with management scenarios including no-tillage and cover crops. For 86 % of grids, maximum erosion rates are simulated under conventional tillage without cover crops. The annual median uncertainty range at each grid due to the choice of erosion equation is 23 t ha^{-1}. In 74 % of grids, the lowest erosion rates were simulated with the MUSS equation. The highest erosion values were simulated with the RUSLE equation (46 %), followed by the USLE equation (25%).

In most locations, the uncertainty due to field management exceeds the uncertainty caused by choice of erosion equation. For 46 % of grids, management scenarios cause the prevailing uncertainty, which we defined as the higher uncertainty range by at least 5 t ha^{-1}. The selected erosion equation causes higher uncertainty by at least 5 t ha^{-1} in 14 % of grids. The map in Figure 4 illustrates the global distribution of prevailing uncertainty sources.

3.2 Main drivers of the global erosion model

We designed the sensitivity study to explain the large variability of simulated water erosion rates in different regions and to discuss the main differences between water erosion equations. Water erosion is highly sensitive to slope steepness (SLP) for all equations. The first-order sensitivity index of the slope parameter indicates that 46–54 % of the variance in the model output is attributable to the slope, without considering interactions between the input parameters (Table 4). Daily precipitation (PRCP) is the second most important parameter for calculating water erosion, with an individual contribution of around 9–20 % to the variance of the output. The remaining parameters contribute together 4–13 % to the output variance.

The first-order sensitivity indices do not include interactions between input parameters, which leads to the sum of all first-order sensitivity indices being lower than 1. The total-order sensitivity indices sum all first-order effects and interactions between parameters, which leads to overlaps in case of interactions and a sum greater than 1. The differences between the first-order and the total-order indices can be used as a measure to determine the impact of the interactions between a specific parameter with other parameters. The total-order sensitivity indices show that slope steepness, including interactions to other parameters, contributes 63–75 % of the output variance from which 18–21 % are due to interactive effects with other parameters (Table 5). The total-order sensitivity indices from precipitation range from 21–36 %, from which 10–18 % is due to interactions with other parameters.

The high sensitivity of slope and precipitation is similar for all equations, but the most sensitive parameters after these can be different for each equation. Equations estimating erosion energy by surface runoff and the RUSLE2 equation are very sensitive to the hydrological soil group (HSG), which determines the soils infiltration ability. This parameter is used in the calculation of the curve number, which defines the partition of precipitation into runoff and infiltration. Also, the land use number (LUN), which is ranked among the most sensitive input parameters, is used for the calculation of the curve number. The most sensitive parameters of the USLE and RUSLE equation, following slope inclination and daily precipitation, are soil texture classes (SAND & SILT) followed by daily temperature changes (TMX). Crop residues (ORHI) are relatively important for all equations but especially important for equations based on rainfall-energy. Other parameters relevant for field management, such as surface roughness and mixing efficiency of the topsoil, have little influence on water erosion.

The sensitivity of slope steepness has a strong positive correlation with the amount of annual precipitation at each location ($\rho = 0.69$, $p<0.01$). The increase in the sensitivity of slope steepness with increasing annual precipitation

https://doi.org/10.5194/bg-2020-93
Preprint. Discussion started: 21 April 2020

is demonstrated in Figure 5, which illustrates substantially lower sensitivity indices at dry locations compared to wet locations. In contrast, the sensitivity indices of daily precipitation are negatively correlated to annual precipitation with a moderate strength ($\rho = 0.45$, $p<0.05$). Depending on the equation, strong positive or negative correlations between SIs and annual precipitation also exist for other parameters such as slope length, soil texture, soil organic carbon, channel length, channel slope and watershed area (Table S4).

3.3 Evaluation of simulation results against field data

The most recent estimated global water erosion rates on cropland of 11 - 13 t ha^{-1} derived from a comparable method (Borrelli et al., 2017; Doetterl et al., 2012; van Oost et al., 2007) lie between our simulated median value of 6 t ha^{-1} and our global average value of 19 t ha^{-1}. In comparison to the median and average values of 473 water erosion measurements of 15 t ha^{-1} and 23 t ha^{-1}, respectively, the global median and average values simulated with our baseline scenario are lower.

To evaluate the agreement between simulated and observed data, we compare median values between simulated and measured erosion rates grouped by precipitation and slope classes, which are defined along the whole range of recorded slope inclinations and annual precipitation amounts of the field data (Figure 6a). Although slope and precipitation classes from the field are spread unevenly, they cover most climatic and topographic characteristics relevant to global agriculture. The comparison illustrates that the deviation between simulated and field data is highest for locations with steep slopes and high annual precipitation. Where slopes are steeper than 8 % and annual precipitation is higher than 1000 mm, the median of simulated water erosion exceeds the median of measured water erosion in most cases by at least 50 t ha^{-1}. With decreasing slope steepness and annual precipitation, the median deviation between simulated and measured data is decreasing. Where both slope steepness is below 8 % and annual precipitation is below 1000 mm, the median deviation is lower than 5 t ha^{1} in most cases. Higher deviations at those locations are caused by simulated water erosion values being lower than measured values. A comparison of measured and simulated water erosion using other equations with the baseline scenario can be found in Fig. S9.

The boxplots in Figure 6b illustrate the range of water erosion values measured in the field and simulated with the baseline scenario. The high median deviation for grouped locations with slopes steeper than 8 % and annual precipitation higher than 1000 mm can also be observed between the range of simulated and measured water erosion values. The range of values at locations with lower precipitation and slope steepness demonstrates that simulated values are mostly below measured values in those environments.

The uncertainty in the choice of management scenarios and water erosion equations included in our baseline scenario leads to an uncertainty of the deviation between simulated and measured erosion values. This uncertainty is demonstrated in Figure 6b by additional three bars illustrating the range of simulated medians defined by minimum and maximum medians stemming from contrasting tillage management scenarios, cover crop scenarios and different water erosion equations. The uncertainty ranges indicate which management scenario and water erosion equation lead to simulation results that agree best with field data for the evaluated slope and precipitation classes.

At locations with low to moderate slope steepness and annual precipitation, the measured water erosion values agree best with the simulation values generated under scenarios implying larger water erosion, such as high

https://doi.org/10.5194/bg-2020-93
Preprint. Discussion started: 21 April 2020

intensity tillage and low soil cover. On the other hand, at locations with steep slopes and intensive precipitation, the measured values are closer to the simulated values under scenarios with less intensive tillage and more soil cover. In addition, the varying sensitivities of each water erosion equation lead to a different magnitude of water erosion values in different environments. On low to moderate slopes, water erosion simulated with the MUSS equation is lowest, whereas RUSLE generates the highest values. On steep slopes, the RUSLE equation generates the lowest water erosion values, which agree best with the measured values. The options to increase and decrease simulated water erosion with different field management scenarios and water erosion equations creates both uncertainty in the model results, but also the possibility to closely match field data.

At locations combining steep slopes and intense precipitation, most management scenarios and equations generate water erosion values that are higher than the measured values. However, those environmental conditions cover only a small share of global cropland. Cultivation areas with slopes steeper than 8 % and annual precipitation higher than 1000 mm represent only 7 % of global maize and wheat cropland in our simulation units. The map in Figure 7 illustrates that the highest concentration of these areas is in East and South-East Asia, followed by Central and South America, and Sub-Saharan Africa.

4 Discussion

Global water erosion estimates generated with an EPIC-based GGCM and our baseline scenario overlap with observed water erosion values under most of the climatic and topographic environments where wheat and maize are grown. However, global wheat and maize land include locations where environmental characteristics differ significantly from the Midwestern United States, where the data was collected to develop the water erosion equations embedded in EPIC. The USLE model and its modification were developed with data for slopes of up to 20 %, which makes model application for steeper slopes uncertain (McCool et al., 1989; Meyer, 1984). Furthermore, the relations between kinetic energy and rainfall energy in the American Great Plains differ from other regions in the world (Roose, 1996). Similarly, the runoff curve number method, which is the key methodology for the calculation of surface runoff, is based on an empirical analysis in watersheds located in the United States and might be less reliable in different regions of the world (Rallison, 1980). Due to the high sensitivity of slope steepness and daily precipitation for the calculation of water erosion, the reliability of the tested equations decreases in regions where typical slope and precipitation patterns differ from the Midwestern US. Although some studies have successfully used USLE and its modification under a different environmental context (e.g. Almas & Jamal, 2009; Sadeghi & Mizuyama, 2007), many studies have concluded that the accuracy of these models may be reduced outside the environments they were created without calibration and model adaptation (e.g. Cohen et al., 2005; Labrière et al., 2015).

The skewed distribution of simulated water erosion values influenced by extreme soil loss rates in few fields highly sensitive to water erosion results in a large difference between the global median of 6 t ha^{-1} a^{-1} and the global average of 19 t ha^{-1} a^{-1}. Due to the strong influence of outliers on average values, the simulated median is a better representation of global and regional water erosion rates in wheat and maize fields. The high sensitivity of the simulation results to slope inclinations and precipitation suggests that a significant share of the estimated soil removal of 7 Gt a^{-1} originates from small wheat and maize fields on steep slopes with strong annual

https://doi.org/10.5194/bg-2020-93
Preprint. Discussion started: 21 April 2020

precipitation. Simulated water erosion values are highly variable depending on the choice of water erosion equation and field management scenario. The water erosion equation chosen for the baseline scenario generates the lowest global soil removal estimate. Different water erosion equations embedded in EPIC estimate a higher global soil removal of up to 11 Gt a^{-1} as well as higher median and average water erosion rates of up to 19 t ha^{-1} a^{-1} and 29 t ha^{-1} a^{-1}. Simulating cover crop and no-tillage worldwide results in the lowest global soil removal of 2 Gt a^{-1} with median and average water erosion rates of 1 and 7 t ha^{-1} a^{-1} and simulating no cover crops and conventional tillage worldwide results in the highest global soil removal of 13 Gt a^{-1} with median and average water erosion rates of 19 and 37 t ha^{-1} a^{-1}. These variations cause uncertainties in the simulation results.

Indeed, a proper reconstruction of a business-as-usual field management is important to narrow down the uncertainty in global crop modelling (Folberth et al., 2019). In this study we allocated a prevailing field management using a set of environmental- and country-specific indicators, similarly to (Porwollik et al., 2019). For example, we accounted for conservation agriculture only in countries where this management strategy is likely. Furthermore, by assuming cover crops in between wheat and maize seasons we simulated more complex cropping systems in the tropics, where long and year-round growing seasons and frequent multi-cropping farm practices barely leave the soil uncovered. Hence, we did not simulate bare fallow in the tropics as erroneously high water erosion values would have been simulated at locations with heavy precipitation falling on bare soil. In addition, conservation practices such as contouring and terracing are crucial to reduce the simulation of high water erosion values on steep slopes. We simulated these practices for specific slope classes under the assumption that farmers around the world uniformly use conservation practices when cultivating on steep slopes. The most relevant parameters used for tillage scenarios are related to crop residues left in the field. In addition, equations directly connected to surface runoff are strongly influenced by the land use number used to determine the impact of cover type and treatment on soil permeability. While both crop residues and green fallow decrease water erosion significantly, especially in the tropics, their use varies widely between regions and even farms, based on a complex web of factors such as institutional factors, farm sizes, risk attitudes, interest rates, access to markets, farming systems, resource endowments, and farm management skills (Pannell et al., 2014). Also, soil conservation measures such as terraces or contour farming significantly influence water erosion but are very heterogeneously used between regions, farming systems and farmers. Our baseline scenario is a very rough depiction of the complex patterns of field management around the world but attempts to represent these highly influential practices with the limited available data.

The MUSS water erosion equation chosen for the baseline scenario generates water erosion rates closest to the field data. The focus of equations on either rainfall energy or runoff energy is relevant for the different simulation results under specific environmental conditions. Equations based on rainfall-energy such as RUSLE and USLE simulate higher water erosion values than the other equations at most locations. However, on steep slopes they generate the lowest water erosion values as runoff becomes a greater source of energy than rain with increasing slope steepness (Roose, 1996). Also, the varying sensitivities of other parameters to the equations such as soil properties and management parameters lead to a varying agreement between simulated and field data depending on the equation selection. Detailed field data would facilitate the choice of an appropriate equation to simulate water erosion worldwide or for a specific region.

https://doi.org/10.5194/bg-2020-93
Preprint. Discussion started: 21 April 2020

418 The selection of field data for evaluating simulated water erosion was limited by the low availability of suitable
419 water erosion observations covering the entire globe. The lack of reliable data on water erosion rates is a severe
420 obstacle for understanding erosion, developing and validating models and implementing soil conservation
421 (Boardman, 2006; Nearing et al., 2000; Poesen et al., 2003; Trimble and Crosson, 2000). The main reasons for
422 the low availability of suitable data to evaluate simulated water erosion rates are twofold: i) erosion monitoring is
423 expensive, time consuming and labour demanding and ii) primary data and metadata of measurement sites
424 accompanying final results are often not available and many older measurements are poorly accessible as they are
425 not available online. Moreover, the geographical distribution of erosion data is unbalanced. Most data are
426 concentrated in the United States, West Europe and the West Mediterranean (García-Ruiz et al., 2015). The
427 appropriate selection of field data to evaluate model outputs needs to be considered as well. At different spatial
428 scales different erosion processes are dominant and consequently different erosion measurement methods are
429 suitable (Boix-Fayos et al., 2006; Stroosnijder, 2005). An overview of erosion methods is provided by Hudson,
430 (1993) and Lal et al. (1994). Recently, most erosion methods are subject of significant criticism (García-Ruiz et
431 al., 2015) and recent development of methodology is in crisis (Stroosnijder, 2005). Most authors use very
432 heterogeneous data sets to evaluate their models, involving data generated by different methods at variable time
433 and spatial scales and variable quality. For example, Doetterl et al. (2012) used plot data, suspended sediments
434 from rivers, and data from RUSLE modelling. Borrelli et al. (2017) used soil erosion rates (measurement methods
435 are not specified), remote sensing, vegetation index (NDVI) and results of RUSLE modelling. In his review on
436 erosion rates under different land use, Montgomery (2007) used field data derived from erosion plots, field-scale
437 measurements, catchment-scale measurements using hydrological methods, ^{137}Cs-method, soil profile truncation
438 and elevated cemetery plots.

439 We decided to use only data obtained by field measurements from erosion plots and by ^{137}Cs method as both
440 methods are most suitable at plot, field and slope scale. Geodetic methods such as erosion pins and laser scanner
441 are also used at these scales, but their accuracy is much lower than the accuracy of plot measurements and ^{137}Cs
442 method. Furthermore, erosion pins are mainly suitable for areas with extreme erosion rates (Hsieh et al., 2009;
443 Hudson, 1993), and laser scanners have difficulties to recognize vegetation (Hsieh et al., 2009). Other commonly
444 used methods such as volumetric method, hydrological method (measurements of discharge and suspended
445 sediment load) and bathymetric method are more suitable for larger scales and the latter two methods involve a
446 significant portion of channel erosion, which is not related with agricultural land (García-Ruiz et al., 2015). We
447 did not consider plot experiments using rainfall simulators as they use artificially generated rainfalls, which mostly
448 have very low energies and thus generate low erosion rates (Boix-Fayos et al., 2006), and usually only small plots
449 are used for rain simulation experiments (García-Ruiz et al., 2015).

450 The evaluation against field measurements in this study provided a first indication of the robustness of results
451 under specific topographic and climatic conditions. However, the reported data does not enable us to further
452 narrow down the uncertainties addressed. Although the metadata accompanying the field measurements includes
453 information on slope steepness and annual precipitation (or geographic coordinates allowing for overlay with
454 climatic data), information on soil types or texture classes, crop type and tillage system implemented over time
455 are provided only for few points. Also, the various methods used to measure erosion rates, their complex
456 implementation and the bias of field studies towards locations sensitive to erosion lead to an uncertain

https://doi.org/10.5194/bg-2020-93
Preprint. Discussion started: 21 April 2020

representation of large-scale erosion rates based on field measurements. To facilitate in-depth evaluation of erosion models across different scales, it is crucial to provide detailed information on site characteristics and to harmonise approaches to measure erosion in the field.

5 Conclusion

The simulation of water erosion with GGCMs is largely influenced by the resolution of global datasets providing topographic, soil, climate, land use and field management data, which is currently not available at the field scale. Yet, considering water erosion in global crop yield projections can provide useful outputs to inform assessments of the potential impacts of erosion on global food production and to identify soil erosion hotspots on cropland for management and policy interventions. To improve the quality of the estimates and to further develop these models, it is crucial to identify, communicate and address the existing uncertainties. Increasing the resolution of global soil, topographic and precipitation data is central for improving global water erosion estimates. In addition, this study provides an insight into the importance of considering field management. The numerous options to simulate the cultivation of fields result in a large range of possible water erosion values, which can only partly be narrowed down at a global scale. Further improvement of global water erosion estimates requires detailed and harmonized field measurements across all environmental conditions to validate and calibrate simulation outputs. Using existing field data, we were able to identify specific environmental characteristics under which the model's performance was not sufficient enough. However, these areas represent only a small fraction of global cropland for wheat and maize. The overlap of simulated and measured water erosion values for most of the global wheat and maize fields underlines the robustness of simulated water erosion values generated with an EPIC-based GGCM.

Data availability. The simulation outputs of the global-gridded EPIC runs are deposited under https://figshare.com/s/ca53095ef7bab516e309 (**temporary link, which will be replaced with a DOI link after revision**). Additional information on model outputs, methods, the study design and the field data are available in the supporting information file: TWCarr-si.zip.

Author contributions. TC, JB, CF and RS designed the study. TC, JB, CF, EF and RS collected and analysed the data. TC prepared the manuscript with contributions from all co-authors.

Competing interests. The authors declare that they have no conflict of interest.

Acknowledgement. This project has received funding from the Grantham Foundation and the European Union's Horizon 2020 research and innovation programme under grant agreement No 776810 (VERIFY) and No 774378 (CIRCASA).

References

Almas, M. and Jamal, T.: Use of RUSLE for Soil Loss Prediction During Different Growth Periods, Pakistan J. Biol. Sci., 3(1), 118–121, doi:10.3923/pjbs.2000.118.121, 2009.

Auerswald, K., Kainz, M. and Fiener, P.: Soil erosion potential of organic versus conventional farming evaluated by USLE modelling of cropping statistics for agricultural districts in Bavaria, Soil Use Manag., 19(4),

305–311, doi:10.1079/sum2003212, 2004.

Balkovič, J., van der Velde, M., Skalský, R., Xiong, W., Folberth, C., Khabarov, N., Smirnov, A., Mueller, N. D. and Obersteiner, M.: Global wheat production potentials and management flexibility under the representative concentration pathways, Glob. Planet. Change, 122, 107–121, doi:10.1016/j.gloplacha.2014.08.010, 2014.

Balkovič, J., Skalský, R., Folberth, C., Khabarov, N., Schmid, E., Madaras, M., Obersteiner, M. and van der Velde, M.: Impacts and Uncertainties of +2°C of Climate Change and Soil Degradation on European Crop Calorie Supply, Earth's Futur., 6(3), 373–395, doi:10.1002/2017EF000629, 2018.

Den Biggelaar, C., Lal, R., Wiebe, K., Eswaran, H., Breneman, V. and Reich, P.: The Global Impact Of Soil Erosion On Productivity*. II: Effects On Crop Yields And Production Over Time, Adv. Agron., 81(03), 49–95, doi:10.1016/S0065-2113(03)81002-7, 2004.

Boardman, J.: Soil erosion science: Reflections on the limitations of current approaches, Catena, 68(2–3), 73–86, doi:10.1016/j.catena.2006.03.007, 2006.

Boix-Fayos, C., Martínez-Mena, M., Arnau-Rosalén, E., Calvo-Cases, A., Castillo, V. and Albaladejo, J.: Measuring soil erosion by field plots: Understanding the sources of variation, Earth-Science Rev., 78(3–4), 267–285, doi:10.1016/j.earscirev.2006.05.005, 2006.

Borrelli, P., Robinson, D. A., Fleischer, L. R., Lugato, E., Ballabio, C., Alewell, C., Meusburger, K., Modugno, S., Schütt, B., Ferro, V., Bagarello, V., Oost, K. Van, Montanarella, L. and Panagos, P.: An assessment of the global impact of 21st century land use change on soil erosion, Nat. Commun., doi:10.1038/s41467-017-02142-7, 2017.

CGIAR-CSI: NASA Shuttle Radar Topographic Mission (SRTM). The SRTM data is available as 3 arc second (approx. 90m resolution) DEMs. The dataset is available for download at: http://srtm.csi.cgiar.org/, 2006.

Chappell, A., Baldock, J. and Sanderman, J.: The global significance of omitting soil erosion from soil organic carbon cycling schemes, Nat. Clim. Chang., 6(2), 187–191, doi:10.1038/nclimate2829, 2016.

Chung, S. W., Gassman, P. W., Kramer, L. A., Williams, J. R., Gu, R. R., Chung, S. W. ;, Gassman, P. W. ;, Kramer, L. A. ; and Williams, J. R. ; Validation of EPIC for Two Watersheds in Southwest Iowa Recommended Citation Validation of EPIC for Two Watersheds in Southwest Iowa, 1999.

Cohen, M. J., Shepherd, K. D. and Walsh, M. G.: Empirical reformulation of the universal soil loss equation for erosion risk assessment in a tropical watershed, Geoderma, 124(3–4), 235–252, doi:10.1016/j.geoderma.2004.05.003, 2005.

Doetterl, S., Van Oost, K. and Six, J.: Towards constraining the magnitude of global agricultural sediment and soil organic carbon fluxes, Earth Surf. Process. Landforms, 37(6), 642–655, doi:10.1002/esp.3198, 2012.

Evans, R. and Boardman, J.: The new assessment of soil loss by water erosion in Europe. Panagos P. et al., 2015 Environmental Science & Policy 54, 438-447-A response, Environ. Sci. Policy, 58, 11–15, doi:10.1016/j.envsci.2015.12.013, 2016.

https://doi.org/10.5194/bg-2020-93
Preprint. Discussion started: 21 April 2020

527 FAO/IIASA/ISRIC/ISSCAS/JRC: Harmonized World Soil Database (version 1.1), 2009.

528 Fick, S. E. and Hijmans, R. .: Worldclim 2: New 1-km spatial resolution climate surfaces for global land areas,
529 Int. J. Climatol., 2017.

530 Fisher, G., Nachtergaele, F., Prieler, S., van Velthuizen, H. T., Verelst, L. and Wiberg, D.: Global Agro-
531 ecological Zones Assessment for Agriculture (GAEZ 2007), IIASA, Laxenburg, Austria and FAO, Rome, Italy.,
532 2007.

533 Folberth, C., Elliott, J., Müller, C., Balkovič, J., Chryssanthacopoulos, J., Izaurralde, R. C., Jones, C. D.,
534 Khabarov, N., Liu, W., Reddy, A., Schmid, E., Skalský, R., Yang, H., Arneth, A., Ciais, P., Deryng, D.,
535 Lawrence, P. J., Olin, S., Pugh, T. A. M., Ruane, A. C. and Wang, X.: Parameterization-induced uncertainties
536 and impacts of crop management harmonization in a global gridded crop model ensemble, PLoS One, 14(9),
537 e0221862, doi:10.1371/journal.pone.0221862, 2019.

538 Fu, B. J., Zhao, W. W., Chen, L. D., Zhang, Q. J., Lü, Y. H., Gulinck, H. and Poesen, J.: Assessment of soil
539 erosion at large watershed scale using RUSLE and GIS: A case study in the Loess Plateau of China, L. Degrad.
540 Dev., 16(1), 73–85, doi:10.1002/ldr.646, 2005.

541 Fulajtar, E., Mabit, L., Renschler, C. S. and Lee Zhi Yi, A.: Use of 137Cs for soil erosion assessment, FAO,
542 Rome., 2017.

543 García-Ruiz, J. M., Beguería, S., Nadal-Romero, E., González-Hidalgo, J. C., Lana-Renault, N. and Sanjuán, Y.:
544 A meta-analysis of soil erosion rates across the world, Geomorphology, 239, 160–173,
545 doi:10.1016/j.geomorph.2015.03.008, 2015.

546 Hsieh, Y. P., Grant, K. T. and Bugna, G. C.: A field method for soil erosion measurements in agricultural and
547 natural lands, J. Soil Water Conserv., 64(6), 374–382, doi:10.2489/jswc.64.6.374, 2009.

548 Hudson, N. W.: Field measurement of soil erosion and runoff, Food and Agriculture Organization of the United
549 Nations, 1993.

550 IIASA/FAO: Global Agro-ecological Zones (GAEZ v3.0), IIASA, Laxenburg, Austria and FAO, Rome, Italy.,
551 2012.

552 Izaurralde, R. C., Williams, J. R., McGill, W. B., Rosenberg, N. J. and Jakas, M. C. Q.: Simulating soil C
553 dynamics with EPIC: Model description and testing against long-term data, Ecol. Modell., 192(3–4), 362–384,
554 doi:10.1016/j.ecolmodel.2005.07.010, 2006.

555 Jenks, G. F.: The Data Model Concept in Statistical Mapping, Int. Yearb. Cartogr., 7, 186–190, 1967.

556 Kaiser, J.: Wounding Earth ' s Fragile Skin, Science (80-.)., 304(June), 1616–1618,
557 doi:10.1126/science.304.5677.1616, 2004.

558 Karydas, C. G., Sekuloska, T. and Silleos, G. N.: Quantification and site-specification of the support practice
559 factor when mapping soil erosion risk associated with olive plantations in the Mediterranean island of Crete,
560 Environ. Monit. Assess., 149(1–4), 19–28, doi:10.1007/s10661-008-0179-8, 2009.

https://doi.org/10.5194/bg-2020-93
Preprint. Discussion started: 21 April 2020

561 Labrière, N., Locatelli, B., Laumonier, Y., Freycon, V. and Bernoux, M.: Soil erosion in the humid tropics: A
562 systematic quantitative review, Agric. Ecosyst. Environ., 203, 127–139, doi:10.1016/j.agee.2015.01.027, 2015.

563 Lal, R.: Soil Erosion Research Methods, 2nd Editio., edited by R. Lal, Taylor & Francis Group., 1994.

564 Luo, Y., Ahlström, A., Allison, S. D., Batjes, N. H., Brovkin, V., Carvalhais, N., Chappell, A., Ciais, P.,
565 Davidson, E. A., Finzi, A., Georgiou, K., Guenet, B., Hararuk, O., Harden, J. W., He, Y., Hopkins, F., Jiang, L.,
566 Koven, C., Jackson, R. B., Jones, C. D., Lara, M. J., Liang, J., McGuire, A. D., Parton, W., Peng, C., Randerson,
567 J. T., Salazar, A., Sierra, C. A., Smith, M. J., Tian, H., Todd-Brown, K. E. O., Torn, M., van Groenigen, K. J.,
568 Wang, Y. P., West, T. O., Wei, Y., Wieder, W. R., Xia, J., Xu, X., Xu, X. and Zhou, T.: Toward more realistic
569 projections of soil carbon dynamics by Earth system models, Global Biogeochem. Cycles, 30(1), 40–56,
570 doi:10.1002/2015GB005239, 2016.

571 Mabit, L., Chhem-Kieth, S., Dornhofer, P., Toloza, A., Benmansour, M., Bernard, C., Fulajtar, E. and Walling,
572 D. E.: 137Cs: A widely used and validated medium-term soil tracer, in Guidelines for using fallout
573 radionuclides to assess erosion and effectiveness of soil conservation strategies. IAEA-TECDOC-1741., pp. 27–
574 78, IAEA, Vienna., 2014.

575 McCool, D. K., Foster, G. R., Mutchler, C. K. and Meyer, L. D.: Revised slope length factor for the Universal
576 Soil Loss Equation, Trans. ASAE, 32, 1571–1576, 1989.

577 McDermid, S. S., Mearns, L. O. and Ruane, A. C.: Representing agriculture in Earth System Models:
578 Approaches and priorities for development, J. Adv. Model. Earth Syst., 9(5), 2230–2265,
579 doi:10.1002/2016MS000749, 2017.

580 Meyer, L. D.: Evolution of the Universal Soil Loss Equation, J. Soil Water Conserv., 39(2), 99–104, 1984.

581 Montgomery, D. R.: Soil erosion and agricultural sustainability., Proc. Natl. Acad. Sci. U. S. A., 104(33),
582 13268–72, doi:10.1073/pnas.0611508104, 2007.

583 Morgan, R. P. C.: Soil erosion and conservation, 3rd ed., Blackwell Science Ltd., 2005.

584 Mueller, C., Elliott, J., Chryssanthacopoulos, J., Arneth, A., Balkovic, J., Ciais, P., Deryng, D., Folberth, C.,
585 Glotter, M., Hoek, S., Iizumi, T., Izaurralde, R. C., Jones, C., Khabarov, N., Lawrence, P., Liu, W., Olin, S.,
586 Pugh, T. A. M., Ray, D. K., Reddy, A., Rosenzweig, C., Ruane, A. C., Sakurai, G., Schmid, E., Skalsky, R.,
587 Song, C. X., Wang, X., De Wit, A. and Yang, H.: Global gridded crop model evaluation: Benchmarking, skills,
588 deficiencies and implications, Geosci. Model Dev., 10(4), 1403–1422, doi:10.5194/gmd-10-1403-2017, 2017.

589 Mueller, N. D., Gerber, J. S., Johnston, M., Ray, D. K., Ramankutty, N. and Foley, J. A.: Closing yield gaps
590 through nutrient and water management, Nature, 494(7437), 390–390, doi:10.1038/nature11907, 2012.

591 Nearing, M. A., Romkens, M. J. M., Norton, L. D., Stott, D. E., Rhoton, F. E., Laflen, J. M., Flanagan, D. C.,
592 Alonso, C. V., Binger, R. L., Dabney, S. M., Doering, O. C., Huang, C. H., McGregor, K. C. and Simon, A.:
593 Measurements and models of soil loss rates, Science (80-.)., 290(5495), 1300–1301, 2000.

594 Nossent, J., Elsen, P. and Bauwens, W.: Sobol' sensitivity analysis of a complex environmental model, Environ.
595 Model. Softw., 26(12), 1515–1525, doi:10.1016/j.envsoft.2011.08.010, 2011.

https://doi.org/10.5194/bg-2020-93
Preprint. Discussion started: 21 April 2020

596 Onstad, C. A. and Foster, G. R.: Erosion modeling on a watershed, Trans. ASAE, 18, 288–292, 1975.

597 Van Oost, K., Quine, T. A., Govers, G., Gryze, S. De, Six, J., Harden, J. W., Mccarty, G. W., Heckrath, G.,
598 Kosmas, C., Giraldez, J. V and Silva, J. R. M.: The Impact of Agricultural Soil Erosion on the Global Carbon
599 Cycle, Science (80-.)., 318(5850), 626–629, 2007.

600 Panagos, P., Borrelli, P., Meusburger, K., van der Zanden, E. H., Poesen, J. and Alewell, C.: Modelling the
601 effect of support practices (P-factor) on the reduction of soil erosion by water at European scale, Environ. Sci.
602 Policy, 51, 23–34, doi:10.1016/j.envsci.2015.03.012, 2015.

603 Panagos, P., Standardi, G., Borrelli, P., Lugato, E., Montanarella, L. and Bosello, F.: Cost of agricultural
604 productivity loss due to soil erosion in the European Union: From direct cost evaluation approaches to the use of
605 macroeconomic models, L. Degrad. Dev., 29(3), 471–484, doi:10.1002/ldr.2879, 2018.

606 Pannell, D. J., Llewellyn, R. S. and Corbeels, M.: The farm-level economics of conservation agriculture for
607 resource-poor farmers, Agric. Ecosyst. Environ., 187, 52–64, doi:10.1016/j.agee.2013.10.014, 2014.

608 Peel, M. C., Finlayson, B. L. and McMahon, T. A.: Updated world map of the Koeppen-Geiger climate
609 classification, Hydrol. Earth Syst. Sci., 11, 1633–1644, doi:10.1097/00041433-200208000-00008, 2007.

610 Pimentel, D.: Soil erosion: A food and environmental threat, Environ. Dev. Sustain., 8(1), 119–137,
611 doi:10.1007/s10668-005-1262-8, 2006.

612 Pimentel, D., Harvey, C., Resosudarmo, P., Sinclair, K., Kurz, D., McNair, M., Crist, S., Shpritz, L., Fitton, L.,
613 Saffouri, R. and Blair, R.: Environmental and economic costs of soil erosion and conservation benefits., Science
614 (80-.)., 267(5201), 1117–1123, doi:10.1126/science.267.5201.1117, 1995.

615 Poesen, J., Nachtergaele, J., Verstraeten, G. and Valentin, C.: Gully erosion and environmental change:
616 Importance and research needs, Catena, 50(2–4), 91–133, doi:10.1016/S0341-8162(02)00143-1, 2003.

617 Pongratz, J., Dolman, H., Don, A., Erb, K. H., Fuchs, R., Herold, M., Jones, C., Kuemmerle, T., Luyssaert, S.,
618 Meyfroidt, P. and Naudts, K.: Models meet data: Challenges and opportunities in implementing land
619 management in Earth system models, Glob. Chang. Biol., 24(4), 1470–1487, doi:10.1111/gcb.13988, 2018.

620 Portmann, F. T., Siebert, S. and Döll, P.: MIRCA2000—Global monthly irrigated and rainfed crop areas around
621 the year 2000: A new high-resolution data set for agricultural and hydrological modeling, Global Biogeochem.
622 Cycles, 24(1), doi:10.1029/2008GB003435, 2010.

623 Porwollik, V., Rolinski, S., Heinke, J. and Müller, C.: Generating a rule-based global gridded tillage dataset,
624 Earth Syst. Sci. Data, 11(2), 823–843, doi:10.5194/essd-11-823-2019, 2019.

625 Rallison, R. E.: Origin and Evolution of the SCS Runoff Equation, in Proceeding of the Symposium on
626 Watershed Management ’80 American Society of Civil Engineering Boise ID., 1980.

627 Renard, K., Foster, G., Weesies, G., McCool, D. and Yoder, D.: Predicting soil erosion by water: a guide to
628 conservation planning with the Revised Universal Soil Loss Equation (RUSLE), Agric. Handb. No. 703, 404,
629 doi:DC0-16-048938-5 65–100., 1997.

https://doi.org/10.5194/bg-2020-93
Preprint. Discussion started: 21 April 2020

630 Roose, E.: Land husbandry - Components and strategy. 70 FAO soils bulletin, Food and Agriculture
631 Organization of the United Nations, Rome., 1996.

632 Ruane, A. C., Goldberg, R. and Chryssanthacopoulos, J.: Climate forcing datasets for agricultural modeling:
633 Merged products for gap-filling and historical climate series estimation, Agric. For. Meteorol., 200, 233–248,
634 doi:10.1016/j.agrformet.2014.09.016, 2015.

635 Sacks, W. J., Deryng, D., Foley, J. A. and Ramankutty, N.: Crop planting dates: An analysis of global patterns,
636 Glob. Ecol. Biogeogr., 19(5), 607–620, doi:10.1111/j.1466-8238.2010.00551.x, 2010.

637 Sadeghi, S. H. R. and Mizuyama, T.: Applicability of the modified universal soil loss equation for prediction of
638 sediment yield in khanmirza watershed, Iran, Hydrol. Sci. Journal-Journal Des Sci. Hydrol., 52(5), 1068–1075,
639 doi:10.1623/hysj.52.5.1068, 2007.

640 Scherer, L. and Pfister, S.: Modelling spatially explicit impacts from phosphorus emissions in agriculture, Int. J.
641 Life Cycle Assess., 20(6), 785–795, doi:10.1007/s11367-015-0880-0, 2015.

642 Sharpley, A. N. and Williams, J. R.: EPIC — Erosion / Productivity Impact Calculator: 1. Model
643 Documentation, U.S. Dep. Agric. Tech. Bull., 1768, 235, 1990.

644 Sobol, I. M.: On sensitivity estimation for nonlinear mathematical models, Matem. Mod., 2, 112–118, 1990.

645 Stroosnijder, L.: Measurement of erosion: Is it possible?, Catena, 64(2–3), 162–173,
646 doi:10.1016/j.catena.2005.08.004, 2005.

647 Terranova, O., Antronico, L., Coscarelli, R. and Iaquinta, P.: Soil erosion risk scenarios in the Mediterranean
648 environment using RUSLE and GIS: An application model for Calabria (southern Italy), Geomorphology,
649 112(3–4), 228–245, doi:10.1016/j.geomorph.2009.06.009, 2009.

650 Trimble, S. W. and Crosson, P.: U.S. Soil Erosion Rates--Myth and Reality, Science (80-.)., 289(5477), 248–
651 250, doi:10.1126/science.289.5477.248, 2000.

652 UN: Standard Country or Area Codes for Statistical Use (Revision 4). Series M, No. 49/Rev.4, New York.,
653 1999.

654 USDA-ARC: Science documentation. Revised Universal Soil Loss Equation, Version 2 (RUSLE 2),
655 Washington, D.C., 2013.

656 USGS: USGS 30 ARC-second Global Elevation Data, GTOPO30, 1997.

657 Våje, P. I., Singh, B. R. and Lal, R.: Soil Erosion and Nutrient Losses from a Volcanic Ash Soil in Kilimanjaro
658 Region, Tanzania, J. Sustain. Agr., 26(4), 23–42, doi:10.1300/J064v26n04, 2005.

659 Walling, D. E. and Webb, B. W.: Erosion and sediment yield: a global overview, IAHS Publ. Proc. Reports-
660 Intern Assoc Hydrol. Sci., 236(236), 3–20, 1996.

661 Walling, D. E., He, Q. and Zhang, Y.: Conversion Models And Related Software, in Guidelines for Using
662 Fallout Radionuclides to Assess Erosion and Effectiveness of Soil Conservation Strategies, IAEA, Vienna.,

https://doi.org/10.5194/bg-2020-93
Preprint. Discussion started: 21 April 2020

2014.

Wang, X., Kemanian, A. R., Williams, J. R., Ahuja, L. R. and Ma, L.: Special Features of the EPIC and APEX Modeling Package and Procedures for Parameterization, Calibration, Validation, and Applications, , 16802, doi:10.2134/advagricsystmodel2.c6, 2011.

Williams, J. R.: Sediment yield prediction with universal equation on using runoff energy factor., in Present and prospective technology for predicting sediment yields and sources, ARS S-40, pp. 244–252, USDA-ARS, Washington.D.C., 1975.

Williams, J. R.: The Erosion-Productivity Impact Calculator (EPIC) Model: A Case History, Philos. Trans. R. Soc. B Biol. Sci., 329(1255), 421–428, doi:10.1098/rstb.1990.0184, 1990.

Williams, J. R.: The EPIC model, in Computer Models of Watershed Hydrology, edited by V. P. Singh, pp. 909–1000, Water Resources Publications., 1995.

Williams, J. R., Izaurralde, R. C. and Steglich, E. M.: Agricultural Policy/Environmental eXtender Model, Theoretical documentation version 0806., 2012.

Wischmeier, W. H. and Smith, D. D.: Predicting rainfall erosion losses, Agric. Handb. no. 537, (537), 285–291, doi:10.1029/TR039i002p00285, 1978.

Zapata, F.: Handbook for the Assessment of Soil Erosion and Sedimentation Using Environmental Radionuclides, Dordrecht., 2002.

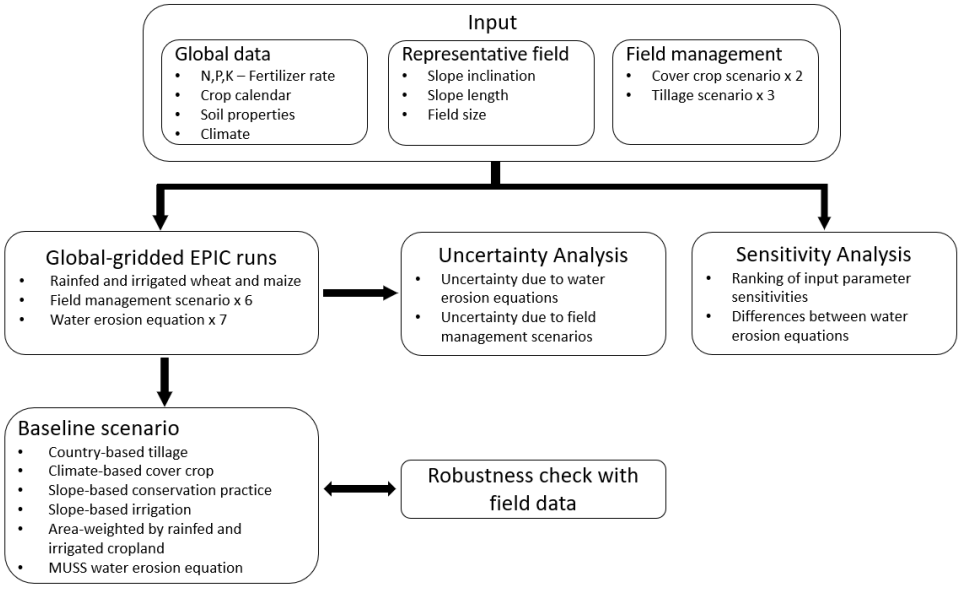

Figure 1: Scheme of procedure used for simulating global water erosion with EPIC-IIASA and for analysing the uncertainty, sensitivity and robustness of our simulation setup.

https://doi.org/10.5194/bg-2020-93
Preprint. Discussion started: 21 April 2020

Biogeosciences
Discussions
Open Access
EGU

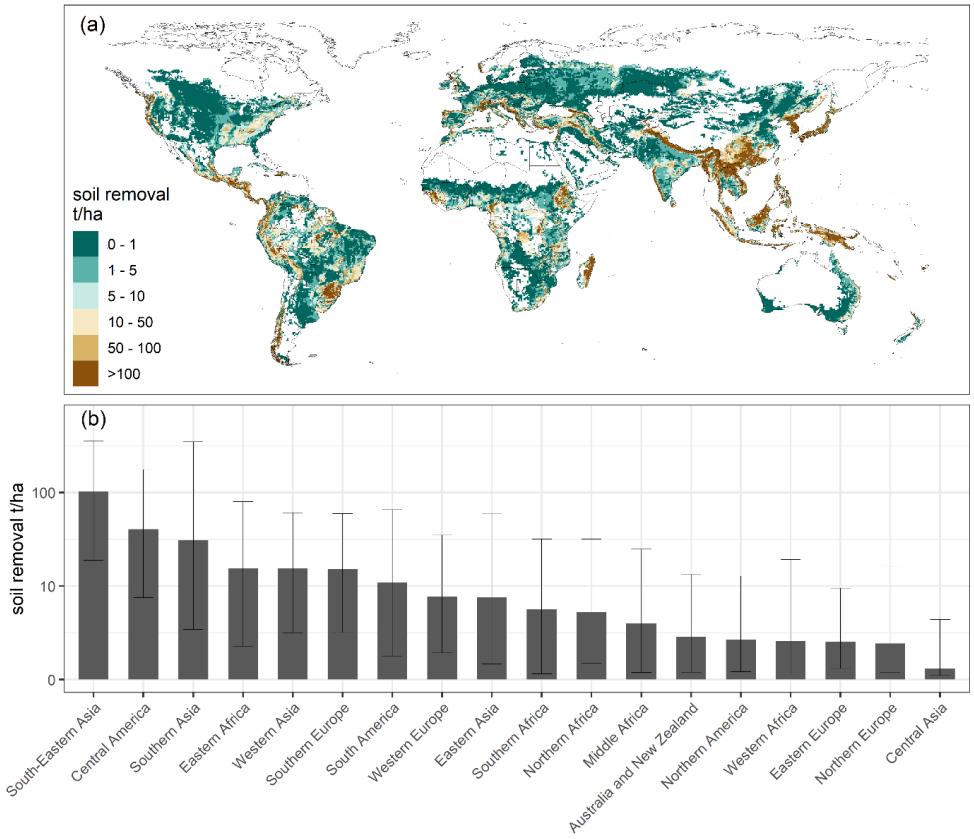

684

685 Figure 2: (a) Soil loss due to water erosion in maize and wheat fields simulated with the baseline scenario. (b)
686 The bars in the bottom plot illustrate the median, the lines and whiskers 25th and 75th percentile of simulated soil
687 loss for major world regions. The classification of world regions is illustrated in Fig. S4. Due to the large gap
688 between aggregated values, all values in the bottom plot have been log-transformed to facilitate the visual
689 comparison.

https://doi.org/10.5194/bg-2020-93
Preprint. Discussion started: 21 April 2020

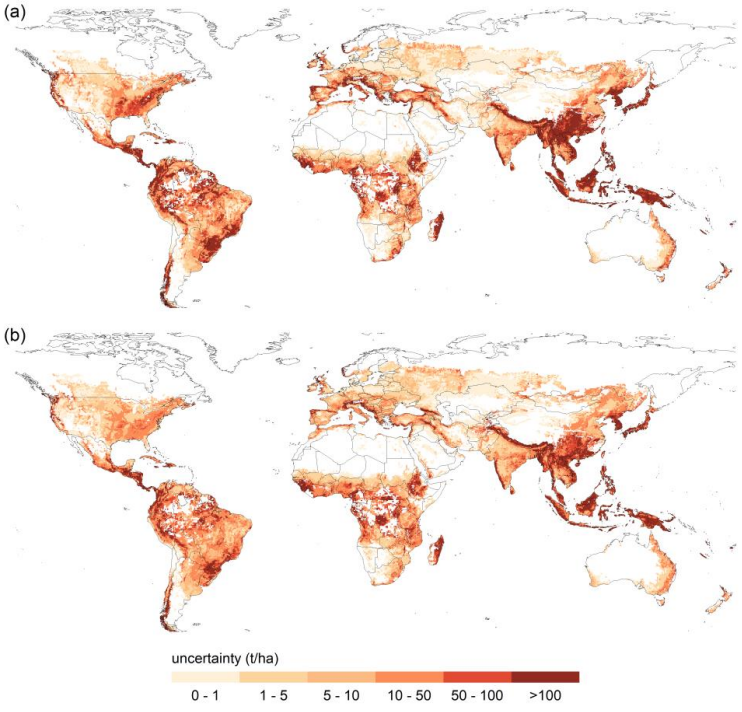

690

691 Figure 3: Water erosion uncertainty due to (a) field management assumptions and (b) water erosion equations.

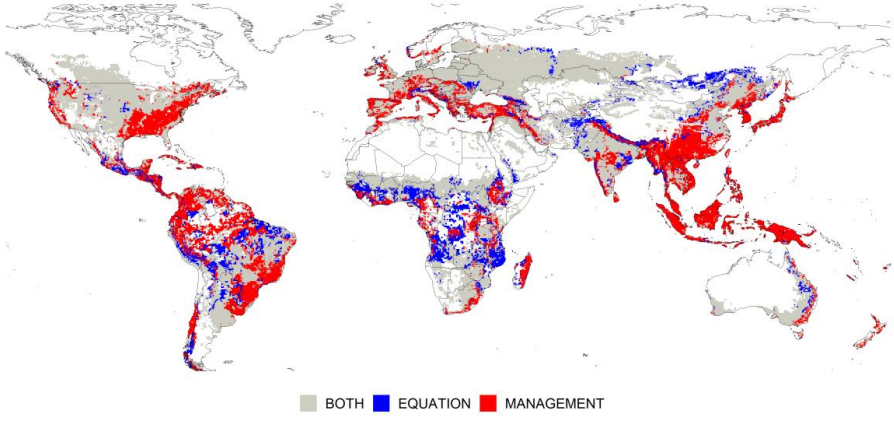

692

693 Figure 4: Prevailing uncertainty, defined as the higher uncertainty range by at least 5 t ha^{-1}.

https://doi.org/10.5194/bg-2020-93
Preprint. Discussion started: 21 April 2020

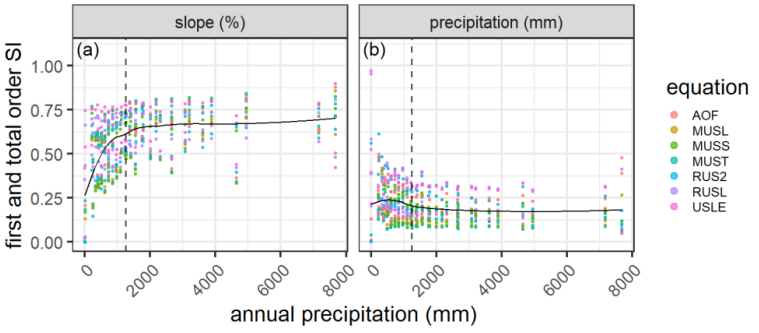

Figure 5: First-order and total-order sensitivity indices (SI) for (a) slope steepness (%) and (b) precipitation [mm]. The dashed vertical line illustrates median annual precipitation at all tested locations (1248 mm).

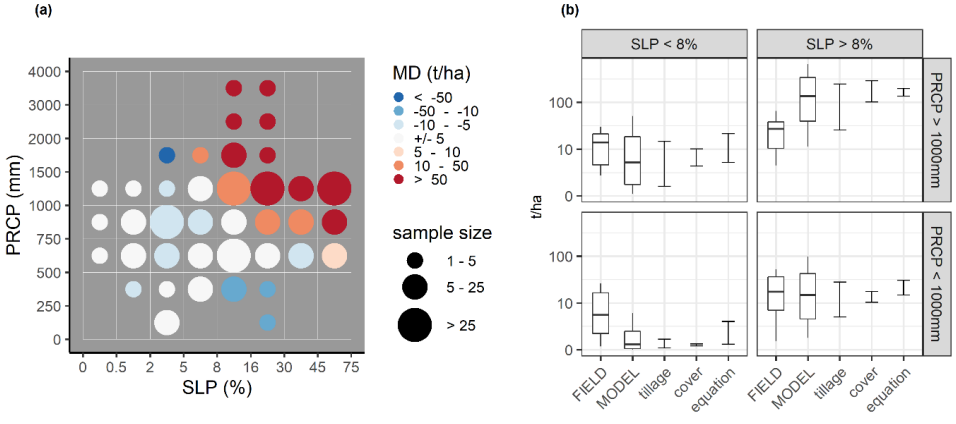

Figure 6: Comparison of simulated erosion with measured erosion. A) Median deviation (MD) in t ha^{1} between simulated erosion using the baseline scenario and measured erosion. Simulated and measured data is grouped into precipitation classes and slope classes used for the simulation setup. B) Measured erosion rates, erosion rates simulated with the baseline scenario and uncertainty ranges for management assumptions and erosion equations. The boxplots are defined by the median, the 25th and the 75th percentile of simulated and measured erosion rates. Whiskers illustrate the 10th and 90th percentile. The three bars next to the boxplots illustrate minimum and maximum median erosion rates calculated with all tillage and cover crop scenarios and with all water erosion equations. The values have been log-transformed for better visualization.

https://doi.org/10.5194/bg-2020-93
Preprint. Discussion started: 21 April 2020

Biogeosciences Discussions
Open Access
EGU

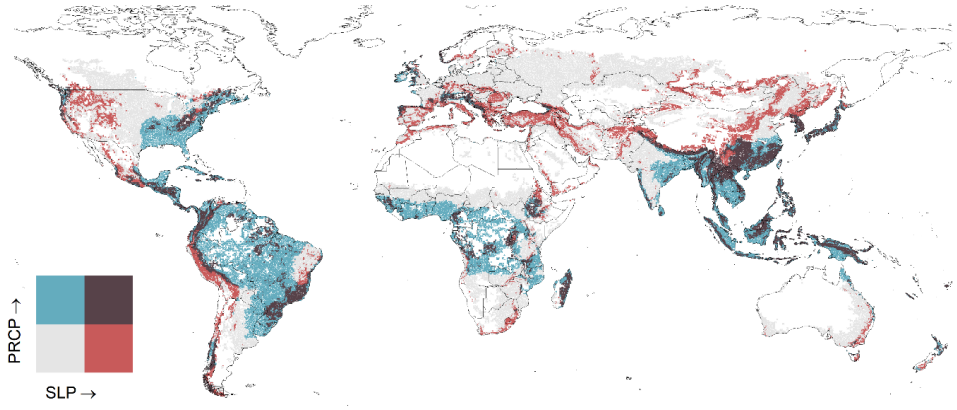

706

707 Figure 7: Distribution of low to high slope steepness (SLP) and annual precipitation (PRCP) in maize and wheat
708 fields. Dark areas illustrate grids where slopes are steeper than 8 % and annual precipitation is above 1000 mm.
709 Correspondingly, blue, red, and grey pixels are below one or both thresholds.

710

711 Table 1: Equations for calculating the erosivity factor in each water erosion equation available in EPIC.

Erosivity factor		**Equation**
$R = EI$	(2)	USLE, RUSLE, RUSLE2 (Renard et al., 1997; USDA-ARC, 2013; Wischmeier and Smith, 1978)
$R = 0.646 * EI + 0.45 * (Q * q_p)^{0.33}$	(3)	AOF (Onstad and Foster, 1975)
$R = 1.586 * (Q * q_p)^{0.56} * WSA^{0.12}$	(4)	MUSLE (Williams 1975)
$R = 2.5 * Q * {q_p}^{0.5}$	(5)	MUST (Williams, 1995)
$R = 0.79 * (Q * q_p)^{0.65} * WSA^{0.009}$	(6)	MUSS (Williams, 1995)

712

713 Table 2: Tillage management scenarios for maize and wheat cultivation

	Conventional tillage	**Reduced tillage**	**No-tillage**
total cultivation operations	6 – 7	4 – 5	3
max. surface roughness	30 – 50 mm	20 mm	10 mm
max. tillage depth	150 mm	150 mm	40 – 60 mm
plant residues left	25 %	50 %	75 %
cover treatment class	straight	contoured	contoured & terraced

714

715 Table 3: Management assumptions and erosion equation selected for the baseline scenario

Option	**Baseline**
TILLAGE	• Mix of conventional, reduced and no-tillage in regions where the national share of conservation agriculture is > 5 % according to the latest reported data in FAO

https://doi.org/10.5194/bg-2020-93
Preprint. Discussion started: 21 April 2020

	AQUASTAT (2007-2014): Argentina, Australia, Bolivia, Brazil, Canada, Chile, China, Colombia, Finland, Italy, Kazakhstan, New Zealand, Paraguay, Spain, USA, Uruguay, Venezuela, Zambia and Zimbabwe. • Mix of conventional and reduced tillage in the rest of the world.			
OFF-SEASON COVER	• Cultivation only with cover crops in tropics according to Koeppen-Geiger regions (Fig. S1) (Peel et al., 2007). • Mix of off-season cover with and without cover crops in temperate and cold zones. • No cover crops in arid regions.			
CONSERVATION PRACTICE FACTOR	Slope	0 – 16 %	16 – 30 %	> 30 %
	P-Factor	1.0	0.5	0.15
CROP	• Water erosion is simulated in wheat and maize fields based on the global crop distribution by MIRCA2000 (Fig. S2) (Portmann et al., 2010). • Weighted average of water erosion under wheat and maize cultivation where both crops are grown.			
IRRIGATION	• Only on slopes ≤ 5 %. • Weighted average of irrigated and rainfed cropland based on MIRCA2000.			
METHOD	MUSS water erosion equation.			

Table 4: First-order sensitivity indices (SI) ranking for the five most sensitive input parameters (PARM) for each water erosion equation including slope steepness (SLP), daily precipitation (PRCP), soil hydrologic group (HSG), land use number (LUN), soil silt content (SILT), soil sand content (SAND), curve number parameter (S301), maximum air temperature (TMX) and crop residues left after harvest (ORHI). The sensitivity indices of the remaining parameters are presented in Table S3.

	AOF		MUSL		MUSS		MUST		RUSLE2		RUSLE		USLE	
rank	**PARM**	**SI**	**PARM**	**SI**	**PARM**	**SI**	**PARM**	**SI**	**PARM**	**SI**	**PARM**	**SI**	**PARM**	**SI**
1	SLP	0.47	SLP	0.47	SLP	0.46	SLP	0.48	SLP	0.46	SLP	0.50	SLP	0.54
2	PRCP	0.13	PRCP	0.10	PRCP	0.12	PRCP	0.09	PRCP	0.16	PRCP	0.20	PRCP	0.18
3	HSG	0.03	HSG	0.04	HSG	0.05	HSG	0.04	HSG	0.03	SAND	0.05	SILT	0.02
4	SILT	0.02	LUN	0.02	LUN	0.02	LUN	0.02	SAND	0.01	TMX	0.01	TMX	0.01
5	LUN	0.01	SILT	0.02	S301	0.01	SILT	0.02	LUN	0.01	ORHI	0.01	ORHI	0.01
…	…	…	…	…	…	…	…	…	…	…	…	…	…	…
sum		0.69		0.68		0.71		0.69		0.71		0.78		0.77

Table 5: Total-order sensitivity indices (SI) ranking for the five most sensitive input parameters (PARM) for each water erosion equation including slope steepness (SLP), daily precipitation (PRCP), soil hydrologic group (HSG), land use number (LUN), soil silt content (SILT), soil sand content (SAND), maximum air temperature (TMX) and crop residues left after harvest (ORHI). The sensitivity indices of the remaining parameters are presented in Table S3.

	AOF		MUSL		MUSS		MUST		RUSLE2		RUSLE		USLE	
rank	**PARM**	**SI**	**PARM**	**SI**	**PARM**	**SI**	**PARM**	**SI**	**PARM**	**SI**	**PARM**	**SI**	**PARM**	**SI**
1	SLP	0.68	SLP	0.68	SLP	0.63	SLP	0.68	SLP	0.66	SLP	0.69	SLP	0.75
2	PRCP	0.28	PRCP	0.23	PRCP	0.22	PRCP	0.21	PRCP	0.32	PRCP	0.36	PRCP	0.36
3	HSG	0.09	HSG	0.12	HSG	0.13	HSG	0.12	HSG	0.08	SAND	0.12	SILT	0.05
4	SILT	0.07	LUN	0.07	LUN	0.07	LUN	0.07	LUN	0.05	TMX	0.02	TMX	0.02
5	LUN	0.05	SILT	0.07	SILT	0.05	SILT	0.07	SAND	0.04	ORHI	0.01	SAND	0.01
…	…	…	…	…	…	…	…	…	…	…	…	…	…	…
sum		1.29		1.30		1.25		1.27		1.34		1.27		1.27